

## Response of genes related to iron and porphyrin transport in *Porphyromonas gingivalis* to blue light



Lintian Yuan<sup>a,g,1</sup>, Yucheng Wang<sup>b,1</sup>, Yanni Zong<sup>c</sup>, Fan Dong<sup>d,g</sup>, Ludan Zhang<sup>e,g</sup>, Guiyan Wang<sup>f,g</sup>, Huihua Dong<sup>d,g</sup>, Yuguang Wang<sup>d,g,\*</sup>

<sup>a</sup> Department of General Dentistry, Peking University School and Hospital of Stomatology, Beijing 100081, PR China

<sup>b</sup> Department of Pharmacology, Institute of Basic Medical Sciences, Chinese Academy of Medical Sciences and School of Basic Medicine, Peking Union Medical College, Beijing 100005, China

<sup>c</sup> Harvard medical school, Boston, MA02115, USA

<sup>d</sup> Center for Digital Dentistry, Peking University School and Hospital of Stomatology, Beijing 100081, PR China

<sup>e</sup> First Clinical Division, Peking University School and Hospital of Stomatology, Beijing 100081, PR China

<sup>f</sup> Department of Pediatric Dentistry, Peking University School and Hospital of Stomatology, Beijing 100081, PR China

<sup>g</sup> National Engineering Research Center of Oral Biomaterials and Digital Medical Devices, Beijing 100081, PR China

### ARTICLE INFO

**Keywords:**

405 nm

Blue light

*Porphyromonas gingivalis*

RNA-seq

ROS

### ABSTRACT

**Background:** Antimicrobial blue light (aBL) kills a variety of bacteria, including *Porphyromonas gingivalis*. However, little is known about the transcriptomic response of *P. gingivalis* to aBL therapy. This study was designed to evaluate the selective cytotoxicity of aBL against *P. gingivalis* over human cells and to further investigate the genetic response of *P. gingivalis* to aBL at the transcriptome level.

**Methods:** Colony forming unit (CFU) testing, confocal laser scanning microscopy (CLSM), and scanning electron microscopy (SEM) were used to investigate the antimicrobial effectiveness of blue light against *P. gingivalis*. The temperatures of the irradiated targets were measured to prevent overheating. Multiple fluorescent probes were used to quantify reactive oxygen species (ROS) generation after blue-light irradiation. RNA sequencing (RNA-seq) was used to investigate the changes in global gene expression. Following the screening of target genes, real-time quantitative polymerase chain reaction (RT-qPCR) was performed to confirm the regulation of gene expression.

**Results:** A 405 nm aBL at 100 mW/cm<sup>2</sup> significantly killed *P. gingivalis* within 5 min while sparing human gingival fibroblasts (HGFs). No obvious temperature changes were detected in the irradiated surface under our experimental conditions. RNA-seq showed that the transcription of multiple genes was regulated, and RT-qPCR revealed that the expression levels of the genes *RgpA* and *RgpB*, which may promote heme uptake, as well as the genes *Ftn* and *FetB*, which are related to iron homeostasis, were significantly upregulated. The expression levels of the *FeoB-2* and *HmuR* genes, which are related to hydroxyl radical scavenging, were significantly downregulated.

**Conclusions:** aBL strengthens the heme uptake and iron export gene pathways while reducing the ROS scavenging pathways in *P. gingivalis*, thus improving the accumulation of endogenous photosensitizers and enhancing oxidative damage to *P. gingivalis*.

### 1. Introduction

*Porphyromonas gingivalis*, a gram-negative bacterium that colonizes the human oral cavity, is involved in the pathogenesis of gingivitis, periodontitis, and peri-implantitis; it is associated with systemic diseases;

and may even promote the development of oral squamous cell carcinoma to some degree [1–5]. The initial therapy for periodontal diseases relies on scaling and root planning, followed by adjunctive therapies, such as antiseptics and/or antibiotics, which may cause brown discoloration of the teeth, alteration in taste, oral mucosal irritation [6–9], or

\* Corresponding author at: Center for Digital Dentistry, Peking University School and Hospital of Stomatology, Beijing 100081, PR China.

E-mail address: [wangyuguang@bjmu.edu.cn](mailto:wangyuguang@bjmu.edu.cn) (Y. Wang).

<sup>1</sup> These authors contributed equally.

drug resistance [10]. Therefore, alternative antimicrobial approaches that target *P. gingivalis* should be explored.

Antibacterial blue light (aBL) in the spectrum of 400–470 nm is a non-antibiotic approach that can selectively kill bacteria while sparing the host cells [11]. Its foundation is comparable to antimicrobial photodynamic therapy [12]. In previous studies, *P. gingivalis* was found to be susceptible to aBL [13–15], and the underlying mechanism was thought to be endogenous photosensitizers such as porphyrins, which can generate cytotoxic reactive oxygen species (ROS) upon blue light irradiation [16]. Considering that *P. gingivalis* lives in an environment covered with fluids orally and oxygen is introduced where the device arrives in clinical periodontal treatment, we need to consider studying the effect of aBL on *P. gingivalis* in an aerobic liquid environment.

Global genome-wide studies on changes in expression patterns in response to antimicrobial agents have provided a deeper understanding of antimicrobial action. In this study, we evaluated the cytotoxicity of aBL on *P. gingivalis* and human gingival fibroblasts (HGFs). Under a suitable light dose that selectively kills bacteria, the genetic response of *P. gingivalis* to aBL was analyzed using RNA-Seq. Analyses of differentially expressed genes (DEGs) showed that aBL regulates the transcription of genes related to heme uptake, iron homeostasis, and hydroxyl radical scavenging. These results were further verified using real-time quantitative polymerase chain reaction (RT-qPCR).

## 2. Materials and Methods

### 2.1. Bacterial Culture

Cryopreserved *P. gingivalis* (W83), generously provided by the Oral Microbiology Laboratory of Peking University School of Stomatology, was resuscitated in brain heart infusion (BHI; Becton, Dickinson and Company, New York, Franklin Lakes, New Jersey, USA) agar medium containing 5% defibrinated sheep blood, 5 µg/mL hemin, and 1 µg/mL vitamin K (Solarbio, Beijing, China). Cells were cultured at 37°C in a BacBasic anaerobic incubator (95% N<sub>2</sub>, 5% CO<sub>2</sub>, and 5% H<sub>2</sub>; SHEL LAB Bactron, Reno, Nevada, USA) for approximately five days to form black colonies.

### 2.2. Light Apparatus

The light source was a blue collimated LED (M405L4, Thorlabs, USA; wavelength 405 ± 8 nm). The power output was measured using a power/energy meter (PM100D; Thorlabs, Newton, NJ, USA). The LED was fixed onto a stand with the light-emitting end right on the top of the bacterial suspension, and the light was delivered vertically to the object. The distance between the light-emitting end and top surface of the bacterial suspension was 3 cm. The irradiance was calculated based on the light output and area of the light spot.

### 2.3. Antimicrobial Blue Light (aBL) Inactivation of bacteria

#### 2.3.1. Colony-forming Unit (CFU) Testing

*P. gingivalis* inoculated from a single colony was cultured in 1 mL of BHI liquid medium overnight and then diluted 1:100 to enrich the culture for approximately 24 h to reach the logarithmic growth phase. The bacterial suspensions were centrifuged, resuspended in phosphate-buffered saline (PBS; P1010; Solarbio, Beijing, China) and adjusted to an optical density of 0.1 at 630 nm (OD<sub>630nm</sub> = 0.1). The suspensions (1 mL) were added to a 12-well plate. For the aBL therapy, an irradiance of 100 mW/cm<sup>2</sup> was used. After exposure to aBL for 0–5 min, each sample was serially diluted 10<sup>1</sup>–10<sup>6</sup> fold with PBS. Aliquots (10 µL) of each dilution were streaked horizontally onto square BHI agar plates and incubated under anaerobic conditions in the dark to allow for colony formation. Each group was tested in triplicates and repeated at least three times.

#### 2.3.2. Confocal Laser Scanning Microscopy (CLSM)

*P. gingivalis* (OD<sub>630nm</sub> = 0.1, 4 mL) was suspended in saline solution and divided into four aliquots in 15 mm glass-bottom cell culture dishes (801,002, NEST, Wuxi, China). The samples were then illuminated with aBL (100 mW/cm<sup>2</sup>) for 0, 5, 10, or 15 min. Each sample was then stained with LIVE/DEAD Bac Light Bacterial Viability stain (L7012, Invitrogen, Carlsbad, CA, USA) following the manufacturer's instructions, and observed under a confocal laser scanning microscope (CLSM, LSM710, Zeiss, Germany). This kit offers two-color discrimination between live and dead populations based on membrane integrity. Cells with intact membranes were stained green (SYTO-9) and considered live, whereas those with compromised membranes were stained red (PI) and considered dead.

#### 2.3.3. Scanning Electron Microscopy (SEM)

*P. gingivalis* (OD<sub>630nm</sub> = 0.1, 300 µL) was suspended in saline solution and subjected to aBL exposure (100 mW/cm<sup>2</sup> for 0 or 15 min). Each sample was fixed with 2.5% glutaraldehyde on a glass sheet at 4°C overnight. The samples were then immersed in 30%, 50%, 70%, 80%, and 90% alcohol for approximately 15 min, followed by two 100% alcohol dehydrations. The samples were air-dried and sputter-coated with metal in vacuum for observation under a scanning electron microscope (SEM; SU8010; Hitachi, Tokyo, Japan).

### 2.4. Safety of Blue Light

#### 2.4.1. Temperature Measurements

To determine whether the efficacy of blue light in killing planktonic bacteria was due to a temperature increase, thermocouples (UT325, UNI-T, Dongguan, China) were used to monitor the temperature changes during blue light irradiation. The temperature was recorded from the time when it reached 36°C and lasted for 720 s (12 min), and the temperature curve was fitted with the Boltzmann function of Origin Pro 2021 (OriginLab Corporation, MA, USA).

#### 2.4.2. Effect of Blue Light on Host Cells Versus bacteria

Human gingival fibroblasts (HGFs) were generously donated by the Central Laboratory of the Peking University School of Stomatology. Cells were grown in antibiotic-free DMEM supplemented with 10% FBS in a 12-well cell culture plate. When cell confluence reached 60%–80%, 10 µL of 10<sup>8</sup> CFU/mL *P. gingivalis* suspension was added to the cell culture and coincubated for 4 h. The mixture was then exposed to aBL at 100 mW/cm<sup>2</sup> for 0 or 5 min. HGF cells not incubated with *P. gingivalis* were used as controls. Live/dead bacterial staining and subsequent fluorescence microscopy (CKX53; olympus, Tokyo, Japan) were used to observe the survival of fibroblasts and bacterial cells.

### 2.5. Reactive Oxygen Species (ROS) Detection

To understand the mechanism underlying aBL inactivation of *P. gingivalis*, we examined ROS production during aBL irradiation using different ROS probe agents:

**Singlet oxygen (<sup>1</sup>O<sub>2</sub>):** Singlet Oxygen Sensor Green (MA0326; Meilunstar, Dalian, China).

**Hydrogen peroxide (H<sub>2</sub>O<sub>2</sub>):** Hydrogen Peroxide Assay Kit (S0038; Beyotime, Shanghai, China).

**Superoxide (O<sub>2</sub><sup>·</sup>):** Superoxide Assay Kit (S0060; Beyotime, Shanghai, China).

**Hydroxyl radicals (·OH):** Hydroxylamine fluorescein (BB-46062; Bestbio, Nanjing, China).

The probes were prepared according to the manufacturers' instructions, and each probe was incubated with the same volume of *P. gingivalis* suspension (10<sup>8</sup> CFU/mL, 100 µL in 96 wells) in PBS for 10 min. Each group was irradiated with aBL for 0–5 min, and fluorescence was measured using a Multimode Plate Reader (Enspire, Perkin Elmer, Waltham, USA) at 1-min intervals. All experiments were performed in

triplicates at least three times.

### 2.6. RNA Sequencing (RNA-seq)

*P. gingivalis* bacterial suspensions were collected as described above and treated with or without aBL. For the aBL-treated group, the basic illumination parameters were the same as those described in Section 2.3.1, except that the exposure time was shortened to 4 min to allow for the presence of live bacteria. The samples were analyzed in triplicate, as shown in Table 1. Transcriptome sequencing and data analyses were performed at the CAS Key Laboratory of Pathogenic Microbiology and Immunology, Institute of Microbiology, Chinese Academy of Sciences. The basic steps included RNA-seq library preparation, sequencing, bioinformatic analysis, and visualization. The details are provided in the Supplementary Materials. Gene Ontology (GO) and Kyoto Encyclopedia of Genes and Genomes (KEGG) enrichment analyses as well as protein-protein interaction (PPI) network analysis were performed.

### 2.7. Reverse Transcription Quantitative Real-time PCR (RT-qPCR)

Total RNA was extracted from *P. gingivalis* using a HiPure Bacterial RNA Kit (R4181; Magen, Guangzhou, China) according to the manufacturer's instructions. The RNA quality was monitored using a UV spectrophotometer (Nanodrop N8000; Thermo Fisher Scientific, USA). All samples used in this study exhibited A260/A280 ratios of 1.8 to 2.1. FastStart Universal SYBR Green Master Mix (ROX) was used for RT-qPCR in Real-Time PCR Systems (Applied Biosystems 7500; Thermo Fisher Scientific company, Cleveland, Ohio, USA) [17]. The primers (Table 2) were designed using Primer 3 (<https://primer3.org/>) and synthesized by Sangon Biotech (Sangon, Shanghai, China). The details are provided in the Supplementary Materials. The resulting fold change represents the relative expression level of a given gene compared to that in the non-irradiated control.

### 2.8. Statistical Analysis

Data were analyzed using the unpaired *t*-test, one-way analysis of variance, or Student's *t*-test when necessary [18–20].  $P < 0.05$  was considered significant. All statistical analyses were performed using Origin Pro (OriginLab Corporation, MA, USA) and Sangerbox 3.0 platform [21].

## 3. Results

### 3.1. The Effect of aBL on *P. gingivalis*

To determine the killing effect of blue light on *P. gingivalis*, bacterial survival after aBL irradiation was observed by the CFU assay and live/dead bacterial staining. CFU testing showed that *P. gingivalis* could achieve  $> 99.9\%$  inactivation after 3–5 min of blue light irradiation (Fig. 1 A). Real-time monitoring of the temperature of the bacterial suspension showed a temperature increase of only 1.7 °C following 5 min of light irradiation, suggesting that the survival loss was unlikely to be attributed to overheating (Fig. 1 B). Although the vast majority of bacteria were unculturable after aBL treatment, the proportion of bacterial cells with compromised membranes accounted for only 15% after

**Table 1**  
Sample information and comparison.

Name	<i>Porphyromonas gingivalis</i> W83 mRNA					
Sample name	BL1	BL2	BL3-r*	C1-r	C2	C3
Sample comparison	BL1/BL2/BL3-r vs C1-r/C2/C3					

\* Grouping symbol “-r” representative sample has rebuilt in the database, only for assuring the accuracy of the samples, no other special meaning.

5 min of irradiation, indicating that most of the cell membrane of *P. gingivalis* remained intact immediately after aBL exposure. After 15 min of irradiation, the proportion of ruptured membranes was  $< 45\%$ , which was inconsistent with the CFU reduction (Fig. 1 C&D). From the SEM images (Fig. 1 E & F), morphological changes in the bacterial cells were also observed after aBL treatment, showing a wrinkled surface or completely broken structure in some of the *P. gingivalis*.

### 3.2. Safety of aBL

The LIVE/DEAD staining using SYTO-9 and PI has been widely used to determine the viability of bacterial cells. In this study, we verified that the stains were also able to distinguish dead cells from living HGF cells (Fig. S2). For irradiation of the HGFs contaminated with *P. gingivalis*, almost all the HGFs were still stained green after 10-min light exposure, indicating that aBL had low toxicity to HGF cells. However, most bacterial cells stained red under the same conditions. The effects of blue light on HGF cells were further determined using the CCK-8 and cell proliferation assays. No significant killing or growth arrest was caused in the HGFs by blue light at 100 mW/cm<sup>2</sup> for 10 min (Fig. S1). Altogether, these results proved that a suitable dosage of aBL could be lethal for *P. gingivalis* but remains safe for host cells (Fig. 2).

### 3.3. ROS Generation Tests

The signals of hydroxyl radicals (-OH) increased by nearly 400% after light irradiation, while those of singlet oxygen (<sup>1</sup>O<sub>2</sub>) and hydrogen peroxide (H<sub>2</sub>O<sub>2</sub>) did not increase significantly. Moreover, the superoxide (O<sub>2</sub><sup>·</sup>) signal unexpectedly declined by  $< 20\%$  (Fig. 3A). The large amount of hydroxyl radical generated led to the speculation that the Fenton reaction, by which free iron catalyzes the conversion of hydrogen peroxides to free radicals, is most likely to be involved in the aBL process. Iron/heme acquisition is an important feature of *P. gingivalis*. Given that hemin may provide the photoactivatable metabolite porphyrins and may also play a protective role against peroxide stress [22], heme homeostasis may be also important in determining aBL efficacy. Therefore, we focused on genes involved in iron and heme metabolism [23–26].

### 3.4. Whole Transcriptional Profile

#### 3.4.1. KEGG Enrichment Results Circle Plot

The KEGG enrichment circle plot was plotted in Sangerbox 3.0 platform, as shown in Fig. 3B. “Metabolic pathways” had the highest score of “Set Size” and “core enrichment”.

#### 3.4.2. GO Pathway

GO analysis of DEGs in *P. gingivalis* subjected to light treatments is shown in the results provided in Fig. 3 C. The main pathway of DEGs in the enrichment of the “cellular component, CC” showed a significant change ( $P_{adjust} < 0.05$ ), especially in the cytoplasmic part. However, neither “biological process, BP” (B& E) nor “molecular function, MF” (C & F) of DEGs enriched were significantly differentially expressed ( $P_{adjust} > 0.05$ ) in Fig. S4.

### 3.5. Differential Gene Screening

To screen out changes in *P. gingivalis* genes caused by aBL, the study first used |fold change|  $\geq 2$  or  $\leq 0.5$  and  $P < 0.05$  as the initial screening conditions. After excluding ribosomal genes, the 26 bases of interest were drawn as protein-protein interactions (PPI) in Fig. 4A using the String system (<https://string-db.org/>).

This study analyzed the results of transcriptome sequencing, starting with genes related to *P. gingivalis* and porphyrin uptake, hydroxyl radical scavenging, and iron transport, and further screened for genes with obvious differential expression. Six representative genes (Fig. 4 B) were selected from RNA-seq data. The RT-qPCR test results are shown in Fig. 4

**Table 2**

Information of genes selected for RT-qPCR.

Gene Number	Gene Name	Primers	
PG_2024	RgpA (hagE)	CGGACAAGGACCGACGAA	TCTGGCCGACTGCACTACC
PG_0506	RgpB (prtRII)	TCACTTGGCACCCTCA	TTCCACCATAGCAAACATACC
PG_1294	FeoB-2	AATCCCAACTGCCGTAAAG	GCTGGAGGGTCAGGTAAA
PG_1552	HmuR	GCACTGGACGGATAAGAT	AGACCCACATTGAGAAGG
PG_1286	Ftn (ferritin)	CGGGAGGTGAAGATAGA	GAAGCAGCCCTACGACA
PG_0669	FetB	TGGCTCGTCTGGTTATA	ACACTCATCAGCGGCATC

C. Compared with the unirradiated control group, the gene expression levels of **RgpA** (PG\_2024, increased 7.41 times), **RgpB** (PG\_0506, increased 8.60 times), **Ftn** (PG\_1286, increased 3.10 times) and **FetB** (PG\_0669, increased 2.39 times) were upregulated after treatment with aBL for 5 min. The expression of the **HmuR** (PG\_1552, retained 0.22 times) and **FeoB-2** (PG\_1294, retained 0.06 times) genes was decreased.

#### 4. Discussion

##### 4.1. The Killing Effect of Blue Light on a *Porphyromonas gingivalis* Suspension in an Aerobic Environment

Some studies on the effects of aBL on *P. gingivalis* were conducted under anaerobic conditions previously. Chui et al. [27] reported that exposure to blue LED only delayed the growth of *P. gingivalis* under anaerobic conditions. RNA degradation and gene expression levels were further examined using the RNA integrity number (RIN) and RT-PCR. Interestingly, genes associated with chromosomal DNA replication and cell division were suppressed at the transcriptional level, which may be the mechanism underlying the bacteriostatic effect of blue light on *P. gingivalis*. In this study, we found that blue light effectively kills *P. gingivalis*, where  $> 3\text{-log CFU}$  reduction could be achieved after 3–5 min of blue light irradiation. This difference may be attributed to the aerobic environment during the light-irradiation process in our experimental setting. The typical oxygen level of periodontal tissue, where *P. gingivalis* resides, is between 3% and 9% [28]. Thereafter, *P. gingivalis* usually lives in a microaerobic environment rather than a completely anaerobic environment. In addition, in the clinical management of *P. gingivalis*-related infections, aBL should be applied post to scaling and root planning procedures, and oxygen can be introduced to the gingival and subgingival tissues during mechanical debridement. Because oxygen may improve aBL effects, we performed light irradiation under normal atmospheric conditions [29].

##### 4.2. Blue Light Can Kill *P. gingivalis* Immediately or Activate Gene Regulation to Cause Death

*P. gingivalis* uses external heme as a source of iron for growth. Its melanin is mainly protoporphyrin IX (PpIX) [30], an endogenous porphyrin that acts as a photosensitizer with a strong absorption peak at 405 nm. *P. gingivalis* was effectively killed by aBL at a low dose in the CFU assay (Fig. 1 A), surprisingly, this lethality did not appear to be caused by the immediate disruption of bacterial cell membranes, as shown by SYTO-9/PI staining (Fig. 1 C&D). SYTO-9 is a green intercalated membrane-permeable stain that can be used to stain any cell that contains nucleic acids, while PI is a red stain that is membrane impermeant and therefore labels only cells with compromised membranes. Because PI has a higher affinity for nucleic acids, when these two stains penetrate a single cell, SYTO-9 is replaced by PI, and the cell appears red [31]. After treatment with aBL for 5 min, only 44% of the bacterial cells stained red, but the CFU assay showed much more prominent killing, indicating that the bacteria may lose viability or reproductivity after the discontinuation of light irradiation.

RNA sequencing has been used extensively in prokaryotes and eukaryotes. For instance, it has been used to study a two-species dynamic

transcriptional model of *P. gingivalis* and *S. gordonii*. Differential genetic analysis suggested that *P. gingivalis* adapted to detoxify peroxides produced by *Streptococcus* [32] and switched between sessile and motile modes in response to environmental and host-related signals [33]. To investigate the metabolic cooperation between *P. gingivalis* and *T. denticola*, RNA-seq was employed to study the transcriptome of *P. gingivalis* exposed to cell-free *T. denticola* [34]. However, to the best of our knowledge, this study is the first to investigate transcriptional changes in *P. gingivalis* exposed to aBL using RNA-seq. Transcripts per million (TPM), reads per kilobase of transcript per million reads mapped (RPKM), and fragments per kilobase of transcript per million reads mapped (FPKM), which account for sequencing depth and feature length, are commonly used to quantify transcript expression levels based on RNA-seq data [35]. In this study, RPKM and FPKM were used for the bioinformatics analysis. Despite the theoretical and practical evidence that the units of mRNA abundance in terms of RPKM or FPKM change between samples [36], the most widely used computational tools by the scientific community continue to measure RNA-Seq abundance in terms of RPKM or FPKM [37–39]. We also compared the results of FPKM with those of TPM and found that they were similar (Fig. S3 B&C). Based on ROS, GO pathway, and KEGG pathway analyses, we identified 26 differentially expressed genes.

The regulation of these genes suggests that the bacteria are confronted with severe stress upon aBL therapy. Some of the genes, such as *SecDF*, *GroEL-ES*, *Ffh*, *PrtRII*, *HtrA*, and *SppA*, are related to protein secretion, folding, translocation or membrane targeting, as well as degradation and refolding of misfolded proteins. *LuxS* is also involved in the activated methyl cycle that is necessary to recycle the metabolite methionine. These are probably responses of cellular repair in the face of oxidative stress. We also noticed that some of the genes are related to bacterial virulence, quorum sensing (QS) or biofilm formation, such as *ClpB*, *SecA*, *ClpX*, *PrtC*, *PrtR*, and *LuxS*. The regulation of these genes suggests that aBL may change the physiopathological processes of bacterial infections in host cells (Table S6).

Of the 26 genes, most are related to cellular protection in response to environmental stress, such as *DnaK*, *ClpB*, *HtpG*, *SecA*, *HtrA*, *PrtRII*, *LuxS*, and *PrtR*. These results are consistent with those of previous studies [27]. Of the 26 genes (Table S6), six, **RgpA**, **RgpB**, **FeoB-2**, **HmuR**, **Ftn**, and **FetB**, were further detected, and RT-qPCR verified that their expression was significantly regulated (Fig. 4C).

##### 4.3. Regulation of Heme and the iron Uptake System Accelerates Death

The heme pigment layer, mainly  $\mu$ -oxobisheme [ $\text{Fe(III)}\text{PpIX}_2\text{O}$ ], can accumulate on the surface of *P. gingivalis* [40]. Arginine-specific gingipain (**Rgp**) and lysine-specific gingipain (**Kgp**) are crucial for forming this pigment layer [41,42]. The heme-binding domain (HA2) of **Kgp** and **RgpA** is capable of binding heme and hemoglobin on the cell surface, and can be used as a catalytic surface for the formation of [ $\text{Fe(III)}\text{PpIX}$ ] 2O and its dimer [43–46]. *P. gingivalis* requires a combination of either or both **RgpA** and **RgpB**, in addition to **Kgp** activity, to produce the -oxo dimer from oxyHb in vitro or during growth on blood-containing media [47]. First, **Rgp** converts oxyhemoglobin into methemoglobin, which is then more susceptible to degradation by **Kgp** protease. **Kgp**-dependent hemin released from hemoglobin is then bound by the hemin/

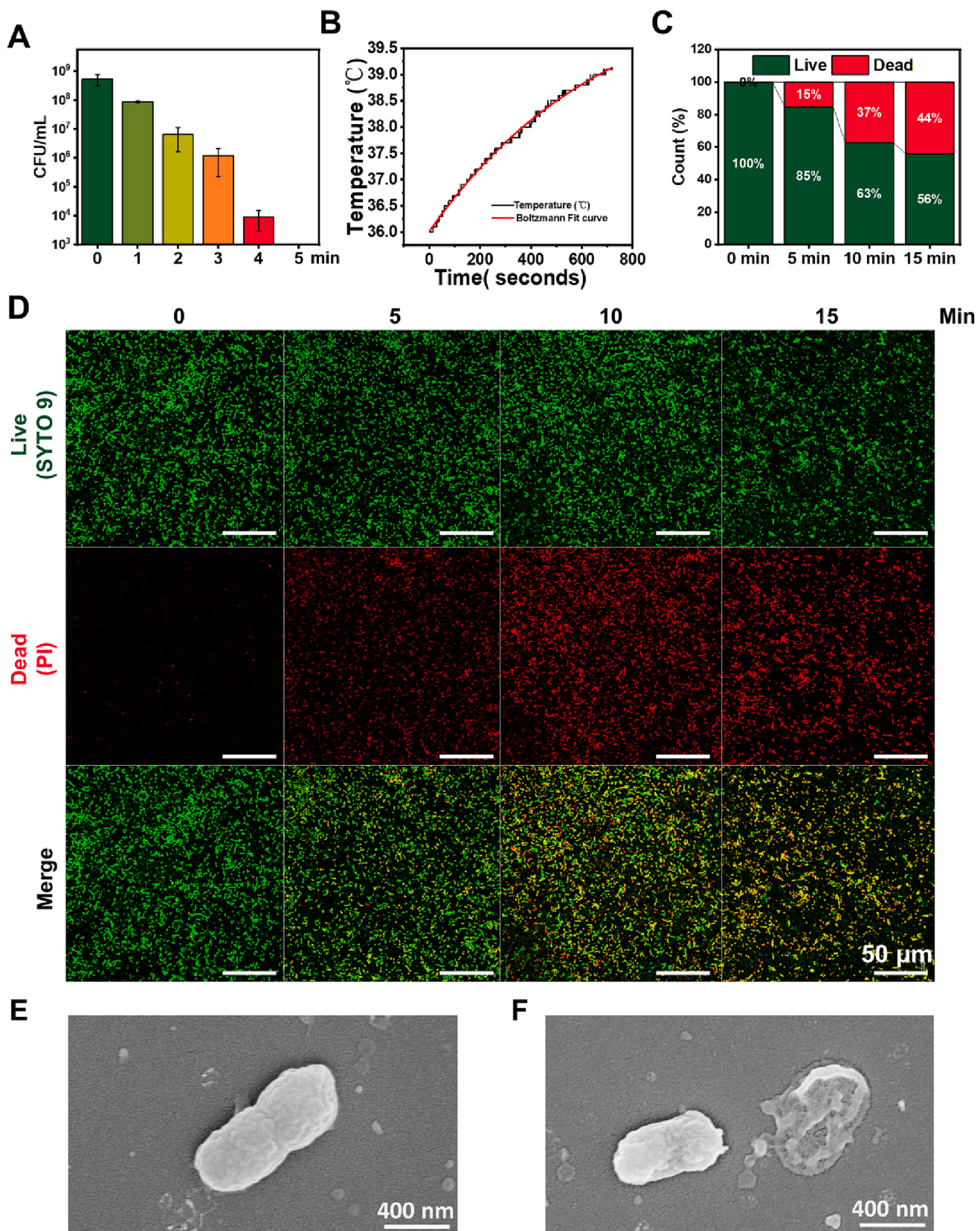


**Fig. 1. The effect of aBL on *P. gingivalis*.** A: CFU assay illustrating the surviving fraction of *P. gingivalis* after treatment with increasing radiant exposure to aBL at 100 mW/cm<sup>2</sup> for 0–5 min. B: Temperature of bacterial suspensions after aBL irradiation. C: Bacterial viability determined using SYTO-9/PI staining and confocal laser scanning microscopy (CLSM). Proportions of bacterial cells that stained green (live) and red (dead) after aBL irradiation for 0–15 min at 100 mW/cm<sup>2</sup>. D: Representative CLSM images illustrating the bacterial viability after aBL treatment at different time points. E&F: Representative SEM images of *P. gingivalis* on glass sheets with (F) or without (E) aBL treatment for 15 min.

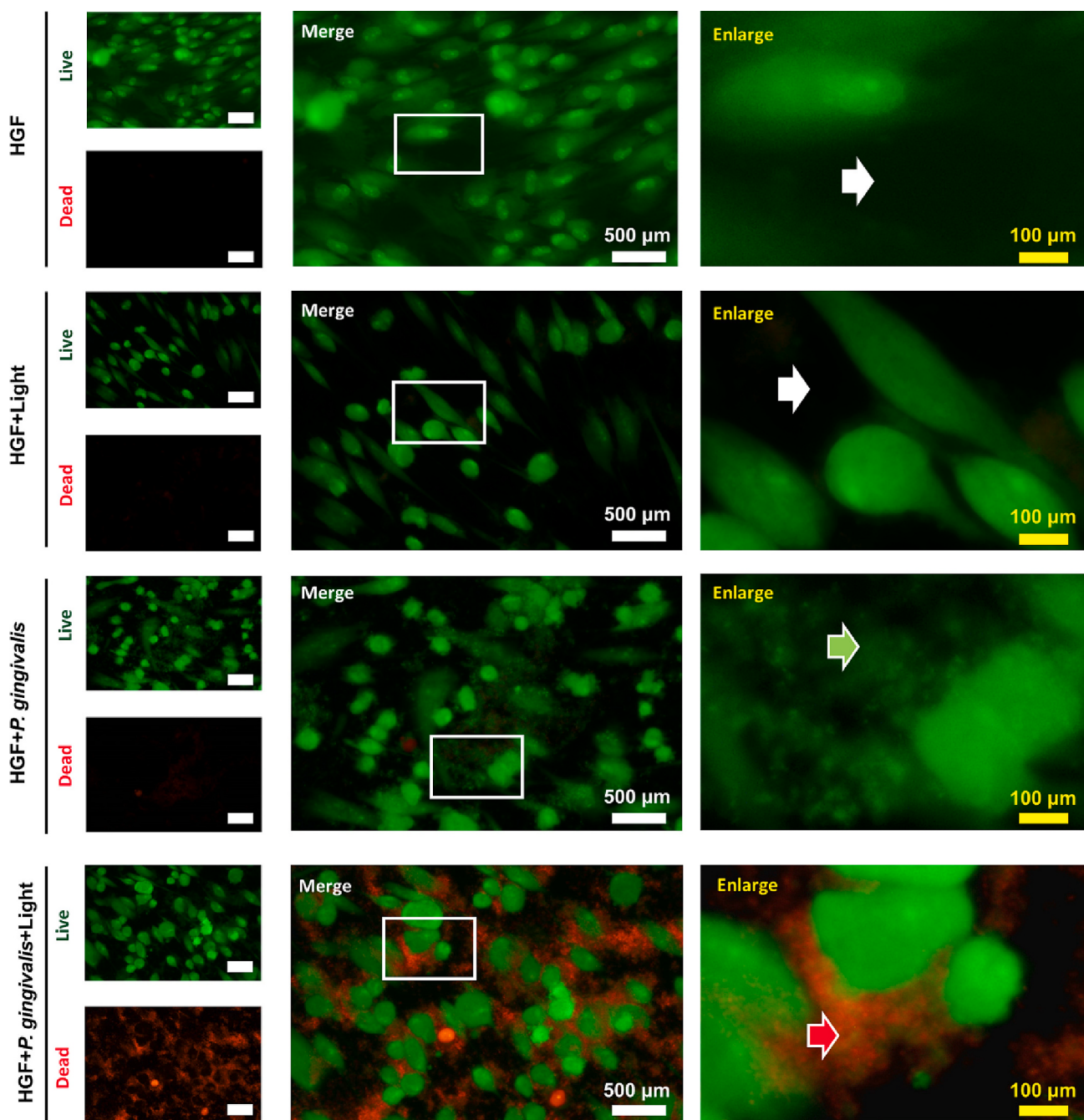


**Fig. 2. Blue light selectively kills *P. gingivalis* while sparing HGF cells.** Cell viability was assessed by SYTO-9/PI staining and fluorescence microscopy. HGF cells, with or without *P. gingivalis* co-incubation, were treated with 100 mW/cm<sup>2</sup> aBL for 0 or 10 min and then stained with SYTO-9/PI. The white arrows show HGF cells without *P. gingivalis* coinubcation. The green arrow shows *P. gingivalis* coinubcated with HGF cells and untreated with aBL. The red arrow shows *P. gingivalis* coinubcated with HGF cells and subsequently exposed to aBL. (For interpretation of the references to color in this figure legend, the reader is referred to the web version of this article.)

hemoglobin receptor and plays a role in the formation of  $\mu$ -oxobishaem. [48–50] (Fig. 5 a). Subsequently, heme uptake system protein A (**HusA**), expressed as an outer membrane protein or released as a soluble protein, can bind heme in monomers and facilitate its transfer to TonB-dependent outer-membrane receptor (**HusB**), allowing the internalization of  $\mu$ -oxobisheme [40,51].

To cope with the ROS generated by aBL treatment, *P. gingivalis* may upregulate antioxidative enzymes, such as heme-dependent catalases, to remove ROS. As expected, during light exposure, the expression of **RgpA** and **RgpB** was upregulated, suggesting an enhanced uptake of heme. However, the heme-derived endogenous photosensitizer PpIX can be

also increased, thus triggering the amplification of bacterial cell death [40].

**FetB** can act as a chelatase, separating iron from heme once heme is taken up by *P. gingivalis* [52]. In *Escherichia coli*, **FetB** was also reported to be involved in iron export [53]. **Ftn** is a well-characterized iron storage protein. It has been linked to iron transport routes and may be more prevalent in pathological conditions, where iron-rich intracellular ferritin is liberated from damaged tissues [54]. The expression of **FetB** [53] and **Ftn** [55] was upregulated after stimulation with aBL, probably because of an increased intracellular heme level. Iron was extracted from the extra heme by **FetB**, subsequently exported by **FetB** and stored

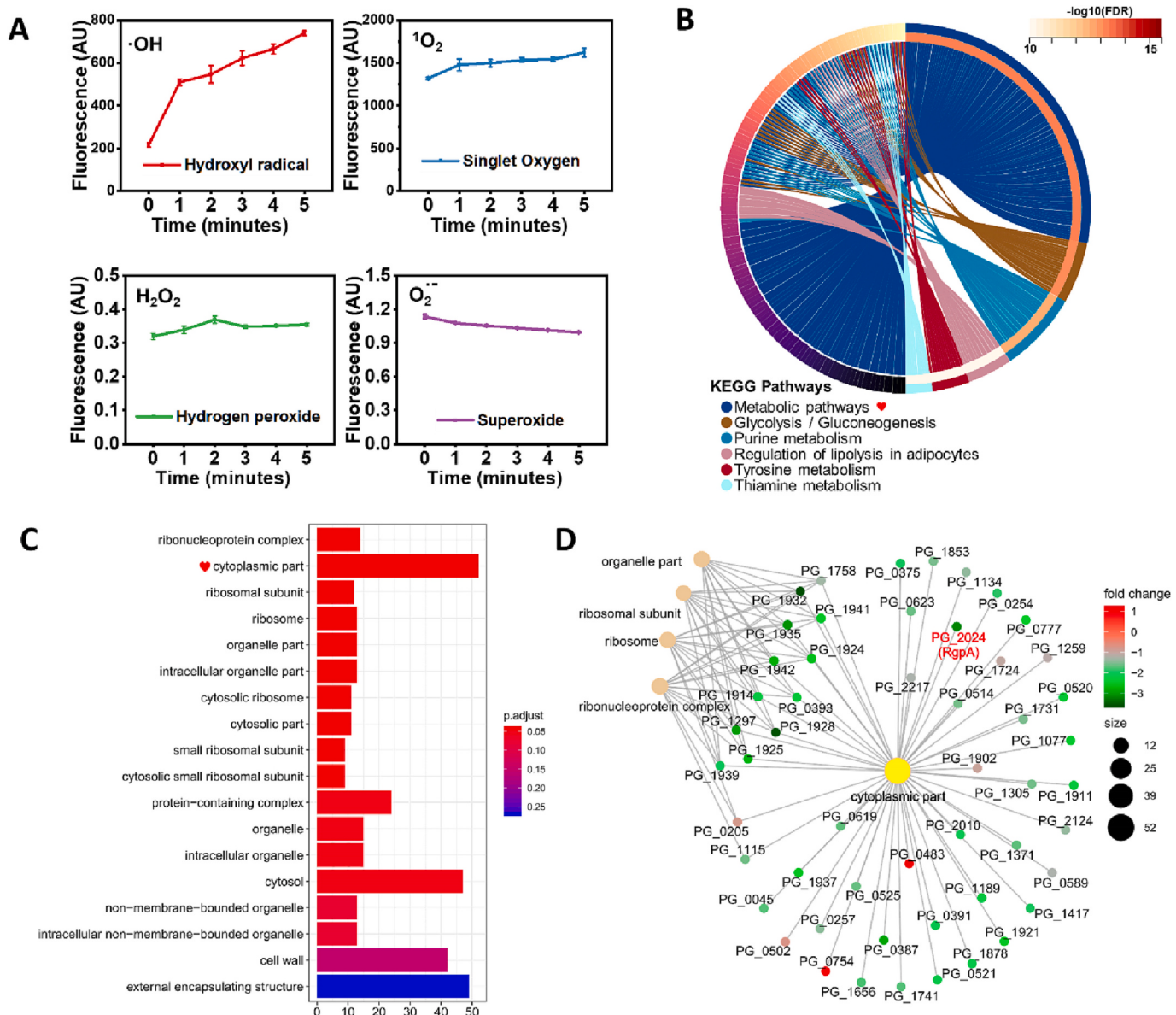


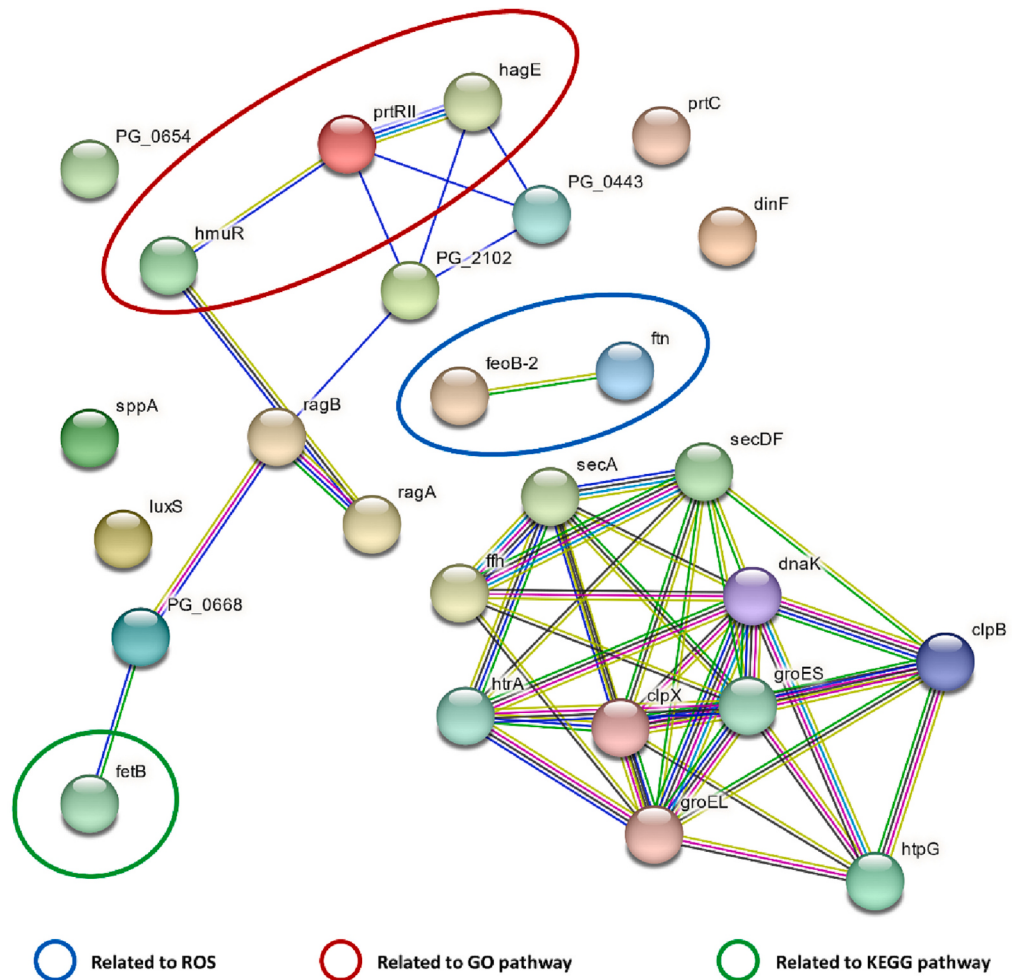
**Fig. 3. GO and KEGG pathways.** A: The signals of the ·OH probe were enhanced with increased aBL exposure. The signals of the  $^1\text{O}_2$  and  $\text{H}_2\text{O}_2$  probes were not obviously increased, and the  $\text{O}_2^-$  signal subsequently declined. B: Enrichment circles of the KEGG pathway. The expression of genes related to metabolic pathways was significantly modified. C: The enriched GO terms for regulated genes in “cellular components”. The color represents the significance of the enriched GO terms. D: The enriched GO terms for regulated genes in the “cytoplasmic part”.

by **Ftn**. The metabolic conversion of ambient oxygen to ROS within bacterial cells can occur when *P. gingivalis* is exposed to the air. During the immunological and inflammatory response, neutrophils and macrophages also create ROS, including H<sub>2</sub>O<sub>2</sub>, by a mechanism known as the “oxidative burst” [56]. Existing research suggests that upon exposure to aBL or ambient oxygen, *P. gingivalis* may accumulate ROS such as H<sub>2</sub>O<sub>2</sub>. Intracellular free iron converts H<sub>2</sub>O<sub>2</sub> into ·OH, which is highly cytotoxic [57]. As shown in Fig. 4A, a significant time-dependent increase in intracellular ·OH was observed after light exposure. The upregulation of **FetB** and **Ftn** is thought to be a protective response of bacteria to reduce free ferrous ions and thus suppress oxidative stress.

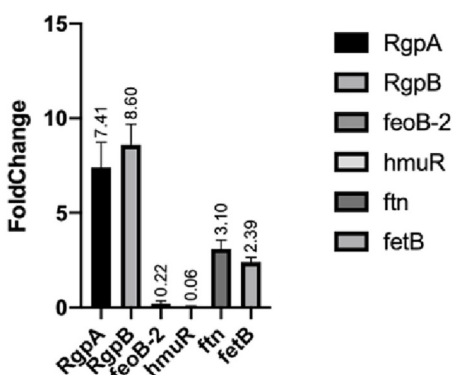
#### **4.4. Downregulated Gene Expression of Manganese and Zinc Transporters under Oxidative Stress Accelerates Death**

Manganese and zinc play significant roles in protecting bacterial pathogens against oxidative stress. First, Mn functions as a cofactor of

enzymes in oxidative stress protection, such as superoxide dismutase (SOD). Second, manganese and zinc can replace iron and copper and are, therefore, more stable and less sensitive to oxidative stress than the latter. ***FeoB-2*** is involved in the transportation of manganese, rather than iron under oxidative stress [58,59]. The TonB-dependent hemoglobin-hemin receptor (***HmuR***) has been reported to be a dual transporter of heme and zinc ions in *Burkholderia thailandensis*, another gram-negative bacterial species. Under normal conditions, it can generally transport heme [60], whereas under oxidative stress, intramolecular disulfide bonds are formed, and zinc ions can be transferred to the cytoplasm [61]. The gene expression levels of ***HmuR*** and ***FeoB-2*** in *P. gingivalis* were significantly reduced following stimulation with aBL, which further reduced the transmembrane transport of zinc and manganese. Such a reduction would block the ROS (particularly ·OH) elimination pathway, ultimately deteriorating oxidative stress and leading to the death of *P. gingivalis*.

**A****B**

Gene functions related to photosensitizers	Gene No.	Gene Name	Fold change	P value
Photosensitizer uptake	PG_2024	RgpA	3.5898	0.01846
	PG_0506	RgpB	0.202545	0.03559
Hydroxyl radical scavenge	PG_1294	feoB2	3.5898	0.01846
	PG_1552	hmuR	2.36142	0.04237
Free iron storage	PG_1286	Ftn	0.35071	0.01880
Prompt iron excess	PG_0669	fetB	0.33433	0.04793

**C**

**Fig. 4. Differential gene screening.** A: Protein-protein interaction (PPI) network of differentially expressed functional genes. Nodes (symbolized as circles) and edges (linking lines) represent DEGs and interactions among DEGs, respectively. Blue circle: gene related to ROS. Red circle: gene related to GO pathway. Green circle: gene related to KEGG pathway. B: RNA-seq of target genes from fine screening. C: RT-qPCR validation results.

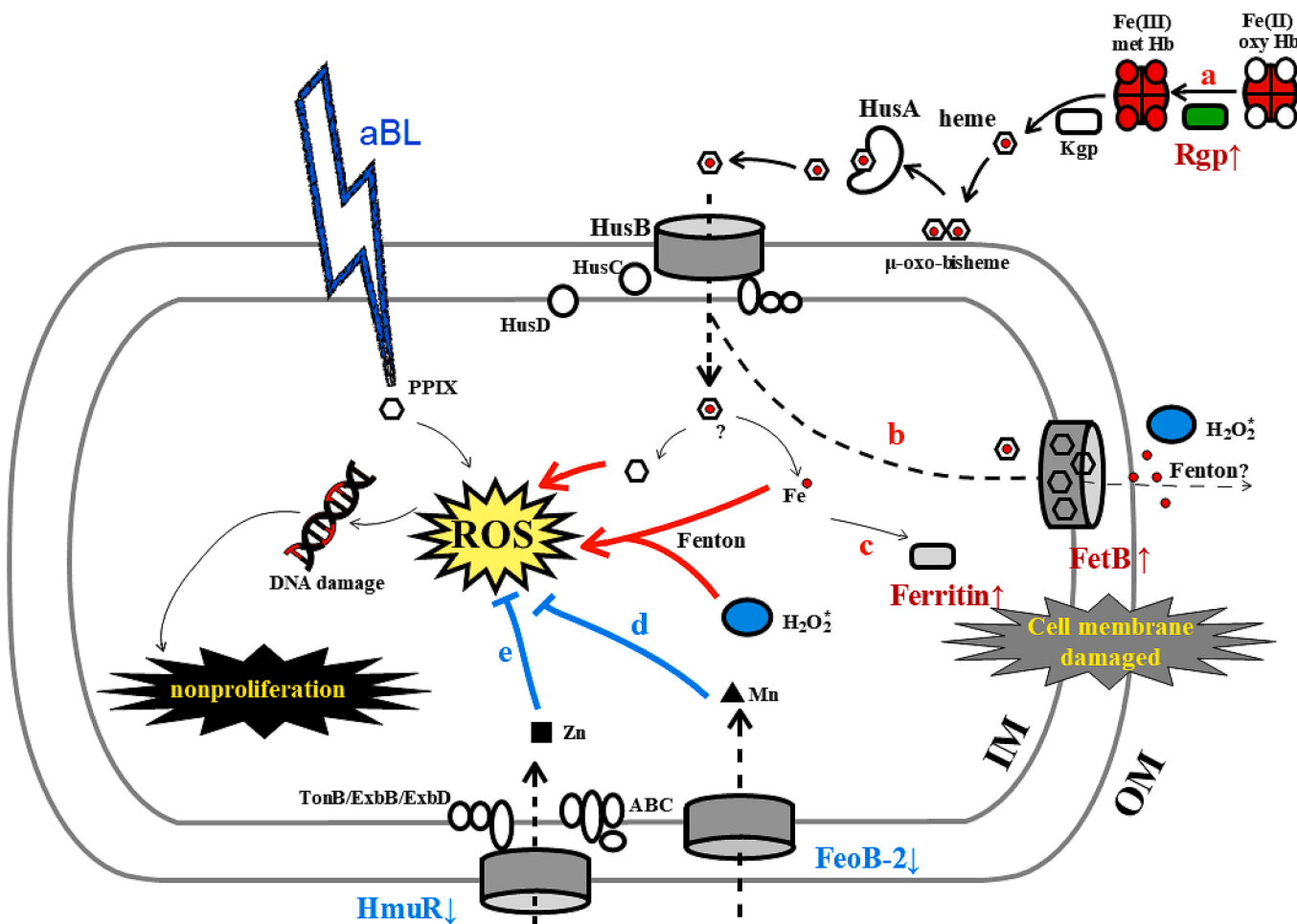


**Fig. 5. Hypothetical mechanism of *P. gingivalis* destruction under aBL stimulus based on the mRNA regulation level.** (a) The upregulated expression of the *RgpA* and *RgpB* genes likely permits the conversion of more oxyhemoglobin to methemoglobin. The degradation of Kgp and transportation of HusA and HusB facilitate the accumulation of intracellular heme, PpIX, and iron. This process potentiates PpIX-induced photosensitization, improves the generation of hydroxyl radicals under aBL irradiation and accelerates the death of *P. gingivalis*. (b, c) The upregulated expression of the *FetB* and *Ftn* genes after aBL irradiation suggests the presence of excess intracellular iron, requiring the feedback upregulation of *FetB* for iron efflux and ferritin for free iron storage. Decreased expression of genes encoding *HmuR* and *FeoB-2* by *FetB* (d, e) may reduce the transmembrane import of zinc and manganese, respectively, thereby blocking the ROS (particularly  $\bullet\text{OH}$ ) elimination pathway and ultimately leading to the death of *P. gingivalis*. (\*)  $\text{H}_2\text{O}_2$  may be produced by *P. gingivalis* in response to ambient oxygen or the cell microenvironment (?): The mechanism remains unknown [40].

## 5. Study Limitations

The present study attributed *P. gingivalis* cell death to ROS generated upon blue light irradiation. Gene regulations may further increase accumulation and reduce scavenging of intracellular ROS, thus potentiate the aBL toxicity. However, it is unclear whether other factors contribute to cell death. More efforts should be made to elucidate factors underlying the mechanism of aBL therapy. In this study, We observed transcriptional changes in heme metabolism, but further evidence is needed to confirm the alterations of iron and heme uptake upon aBL therapy in *P. gingivalis*, as transcriptional changes do not always align with functional changes. Future research will focus on the changes in the molecular composition of intracellular components. Although different sets of genes could be regulated in response to blue light, only six selected genes were validated with qRT-PCR. There are still a great number of other genes that can be good candidates for further mining and investigation.

## 6. Conclusion

The aBL of appropriate parameters can effectively kill planktonic *P. gingivalis* while appearing to be safe for host cells. It may deactivate

*P. gingivalis* by inducing ROS production from endogenous photosensitizers. Although multiple ROS may account for the aBL effect, hydroxyl radicals may play an important role in killing *P. gingivalis*. aBL triggers *P. gingivalis* to import excess heme as a coenzyme into antioxidant enzymes. However, aBL can activate heme-derived PpIX to form ROS, thus killing *P. gingivalis* in a “chain reaction.” Therefore, aBL may be an effective treatment for *P. gingivalis* infection-related dental diseases.

## Author Statements

Lintian Yuan: Methodology, Formal analysis, writing.  
 Yucheng Wang: Methodology and Writing – Review & Editing.  
 Yanni Zong: PCR experiments and analysis.  
 Fan Dong: Safety experiments and analysis.  
 Ludan Zhang: Bacterial experiments and analysis.  
 Guiyan Wang: Writing – Review & Editing.  
 Huihua Dong: Text checking.  
 Yuguang Wang: Conceptualization, Resources, Writing – Review & Editing and Funding acquisition.

## Declaration of Competing Interest

The authors declare that they have no known competing financial interests or personal relationships that could have appeared to influence the work reported in this paper.

## Data availability

The authors are unable or have chosen not to specify which data has been used.

## Acknowledgments

This work was supported by grants from the Fundamental Research Funds for the Central Universities-Peking University Medicine Fund of Fostering Young Scholars' Scientific & Technological Innovation (BMU2022PYB032) and the National Natural Science Foundation of China (52271127, Yuguang wang) and (82002094, Yucheng wang).

## Appendix A. Supplementary data

Supplementary data to this article can be found online at <https://doi.org/10.1016/j.jphotobiol.2023.112670>.

## References

- [1] K.Y. How, K.P. Song, K.G. Chan, Porphyromonas gingivalis: an overview of periodontopathic pathogen below the gum line, *Front. Microbiol.* 7 (2016) 53.
- [2] C.J. Carter, J. France, S. Crean, S.K. Singhrao, The Porphyromonas gingivalis/host Interactome shows enrichment in GWASdb genes related to Alzheimer's disease, diabetes and cardiovascular diseases, *Front. Aging Neurosci.* 9 (2017).
- [3] C. Damgaard, J. Reinholdt, C. Enevold, Immunoglobulin G antibodies against Porphyromonas gingivalis or Aggregatibacter actinomycetemcomitans in cardiovascular disease and periodontitis (vol 9, 1374154, 2017), *J. Oral. Microbiol.* 10 (2018).
- [4] I. Olsen, S.K. Singhrao, Is there a link between genetic defects in the complement cascade and Porphyromonas gingivalis in Alzheimer's disease? *J. Oral. Microbiol.* 12 (2020).
- [5] P. Radhakrishnan, R. Anbalagan, R. Barani, M. Mani, K.G. Seshadri, P. Srikanth, Sequencing of Porphyromonas gingivalis from saliva in patients with periodontitis and type 2 diabetes mellitus, *Indian J. Med. Microbiol.* 37 (2019) 54–59.
- [6] T.M. Karpinski, A.K. Szkaradkiewicz, Chlorhexidine—pharmacological activity and application, *Eur. Rev. Med. Pharmacol. Sci.* 19 (2015) 1321–1326.
- [7] J.F. Gent, M.E. Frank, T.P. Hettinger, Taste confusions following chlorhexidine treatment, *Chem. Senses* 27 (2002) 73–80.
- [8] N.L. Plantinga, B.H.J. Wittekamp, K. Leleu, P. Depuydt, A.M. Van den Abeele, C. Brun-Buisson, M.J.M. Bonten, Oral mucosal adverse events with chlorhexidine 2% mouthwash in ICU, *Intensive Care Med.* 42 (2016) 620–621.
- [9] S. Takenaka, M. Sotozono, N. Ohkura, Y. Noiri, Evidence on the use of mouthwash for the control of supragingival biofilm and its potential adverse effects, *Antibiotics (Basel)* 11 (2022).
- [10] L. Brooks, U. Narvekar, A. McDonald, P. Mullany, Prevalence of antibiotic resistance genes in the oral cavity and mobile genetic elements that disseminate antimicrobial resistance: a systematic review, *Mol Oral Microbiol* 37 (2022) 133–153.
- [11] Y. Wang, R. Ferrer-Espada, Y. Baglo, Y. Gu, T. Dai, Antimicrobial blue light inactivation of neisseria gonorrhoeae: roles of wavelength, endogenous photosensitizer, oxygen, and reactive oxygen species, *Lasers Surg. Med.* 51 (2019) 815–823.
- [12] L. Yuan, P. Lyu, Y.Y. Huang, N. Du, W. Qi, M.R. Hamblin, Y. Wang, Potassium iodide enhances the photobactericidal effect of methylene blue on enterococcus faecalis as planktonic cells and as biofilm infection in teeth, *J. Photochem. Photobiol. B* 203 (2020), 111730.
- [13] C.R. Fontana, X. Song, A. Polymeri, J.M. Goodson, X. Wang, N.S. Soukos, The effect of blue light on periodontal biofilm growth in vitro, *Lasers Med. Sci.* 30 (2015) 2077–2086.
- [14] N.S. Soukos, J. Stultz, A.D. Abernethy, J.M. Goodson, Phototargeting human periodontal pathogens in vivo, *Lasers Med. Sci.* 30 (2015) 943–952.
- [15] S. Shany-Kdoshim, D. Polak, Y. Houri-Haddad, O. Feuerstein, Killing mechanism of bacteria within multi-species biofilm by blue light, *J. Oral. Microbiol.* 11 (2019) 1628577.
- [16] Y. Wang, Y. Wang, Y. Wang, C.K. Murray, M.R. Hamblin, D.C. Hooper, T. Dai, Antimicrobial blue light inactivation of pathogenic microbes: state of the art, *Drug Resist. Updat.* 33–35 (2017) 1–22.
- [17] X.Y. Meng, Y.S. Li, Y. Zhou, Y.Y. Zhang, B. Qiao, Y. Sun, L. Yang, P. Hu, S.Y. Lu, H. L. Ren, J.H. Zhang, X.R. Wang, Z.S. Liu, Real-time immuno-PCR for ultrasensitive detection of pyrene and other homologous PAHs, *Biosens. Bioelectron.* 70 (2015) 42–47.
- [18] S. Shany-Kdoshim, D. Polak, Y. Houri-Haddad, O. Feuerstein, Killing mechanism of bacteria within multi-species biofilm by blue light, *J. Oral. Microbiol.* 11 (2019).
- [19] W. Luo, R.S. Liu, J.G. Zhu, Y.C. Li, H.C. Liu, Subcellular location and photodynamic therapeutic effect of chlorin e6 in the human tongue squamous cell cancer Te8113 cell line, *Oncol. Lett.* 9 (2015) 551–556.
- [20] K. Lee, J.S. Roberts, C.H. Choi, K.R. Atanasova, O. Yilmaz, *Porphyromonas gingivalis* traffics into endoplasmic reticulum-rich-autophagosomes for successful survival in human gingival epithelial cells, *Virulence* 9 (2018) 845–859.
- [21] W. Shen, Z. Song, X. Zhong, M. Huang, D. Shen, P. Gao, X. Qian, M. Wang, X. He, T. Wang, S. Li, X. Song, Sangerbox: A comprehensive, interaction-friendly clinical bioinformatics analysis platform, *iMeta* 1 (2022), e36.
- [22] J.W. Smalley, A.J. Birss, J. Silver, The periodontal pathogen *Porphyromonas gingivalis* harnesses the chemistry of the mu-oxo bisheme of iron protoporphyrin IX to protect against hydrogen peroxide, *FEMS Microbiol. Lett.* 183 (2000) 159–164.
- [23] A. Yoshida, H. Sasaki, T. Toyama, M. Araki, J. Fujioka, K. Tsukiyama, N. Hamada, F. Yoshino, Antimicrobial effect of blue light using *Porphyromonas gingivalis* pigment, *Sci. Rep.* 7 (2017) 5225.
- [24] A. Wissbrock, A.A. Paul George, H.H. Brewitz, T. Kuhl, D. Imhof, The molecular basis of transient heme-protein interactions: analysis, concept and implementation, *Biosci. Rep.* 39 (2019).
- [25] A. Sikora, A.M. Maciejewska, J. Poznanski, T. Pilzys, M. Marcinkowski, M. Dylewska, J. Piwowarski, W. Jakubczak, K. Pawlak, E. Grzesiuk, Effects of changes in intracellular iron pool on AlkB-dependent and AlkB-independent mechanisms protecting *E.coli* cells against mutagenic action of alkylating agent, *Mutat. Res.* 778 (2015) 52–60.
- [26] B. Wang, X. Zhang, W. Fang, C. Rovira, S. Shaik, How do Metalloproteins tame the Fenton reaction and utilize ·OH radicals in constructive manners? *Acc. Chem. Res.* 55 (2022) 2280–2290.
- [27] C. Chui, K. Hiratsuka, A. Aoki, Y. Takeuchi, Y. Abiko, Y. Izumi, Blue LED inhibits the growth of *Porphyromonas gingivalis* by suppressing the expression of genes associated with DNA replication and cell division, *Lasers Surg. Med.* 44 (2012) 856–864.
- [28] K.A. Thomas, Angiogenesis, in: R.A. Bradshaw, P.D. Stahl (Eds.), *Encyclopedia of Cell Biology*, Academic Press, Waltham, 2016, pp. 102–116.
- [29] K. Abed, N. Moubayed, M.S. BinShabaib, A.L. SS, Is a single session of antimicrobial photodynamic therapy as an adjuvant to non-surgical scaling and root planing effective in reducing periodontal inflammation and subgingival presence of *Porphyromonas gingivalis* and *Aggregatibacter actinomycetemcomitans* in patients with periodontitis? *Photodiagn. Photodyn. Ther.* 38 (2022), 102847.
- [30] J.W. Smalley, J. Silver, P.J. Marsh, A.J. Birss, The periodontopathogen *Porphyromonas gingivalis* binds iron protoporphyrin IX in the mu-oxo dimeric form: an oxidative buffer and possible pathogenic mechanism, *Biochem. J.* 331 (1998) 681–685.
- [31] S.M. Stocks, Mechanism and use of the commercially available viability stain, *BacLight*, *Cytometry A* 61 (2004) 189–195.
- [32] E.L. Hendrickson, D.A. Beck, D.P. Miller, Q. Wang, M. Whiteley, R.J. Lamont, M. Hackett, Insights into dynamic polymicrobial synergy revealed by time-coursed RNA-Seq, *Front. Microbiol.* 8 (2017) 261.
- [33] D.M. Vermilyea, M.F. Moradali, H.M. Kim, M.E. Davey, PPAD activity promotes outer membrane vesicle biogenesis and surface translocation by porphyromonas gingivalis, *J. Bacteriol.* 203 (2021).
- [34] L.X. Kin, C.A. Butler, N. Slakeski, B. Hoffmann, S.G. Dashper, E.C. Reynolds, Metabolic cooperativity between *Porphyromonas gingivalis* and *Treponema denticola*, *J. Oral. Microbiol.* 12 (2020) 1808750.
- [35] A. Conesa, P. Madrigal, S. Tarazona, D. Gomez-Cabrero, A. Cervera, A. McPherson, M.W. Szczesniak, D.J. Gaffney, L.L. Elo, X. Zhang, A. Mortazavi, A survey of best practices for RNA-seq data analysis, *Genome Biol.* 17 (2016) 13.
- [36] G.P. Wagner, K. Kin, V.J. Lynch, Measurement of mRNA abundance using RNA-seq data: RPKM measure is inconsistent among samples, *Theory Biosci.* 131 (2012) 281–285.
- [37] R. Vera Alvarez, L.S. Pongor, L. Marino-Ramirez, D. Landsman, TPMCalculator: one-step software to quantify mRNA abundance of genomic features, *Bioinformatics* 35 (2019) 1960–1962.
- [38] D. Peng, C. Ruan, S. Fu, C. He, J. Song, H. Li, Y. Tu, D. Tang, L. Yao, S. Lin, Y. Shi, W. Zhang, H. Zhou, L. Zhu, C. Ma, C. Chang, J. Ma, Z. Xie, C. Wang, Y. Xue, Atg9-centered multi-omics integration reveals new autophagy regulators in *Saccharomyces cerevisiae*, *Autophagy* 17 (2021) 4453–4476.
- [39] C. Ruan, C. Wang, X. Gong, Y. Zhang, W. Deng, J. Zhou, D. Huang, Z. Wang, Q. Zhang, A. Guo, J. Lu, J. Gao, D. Peng, Y. Xue, An integrative multi-omics approach uncovers the regulatory role of CDK7 and CDK4 in autophagy activation induced by silica nanoparticles, *Autophagy* 17 (2021) 1426–1447.
- [40] J.W. Smalley, T. Olczak, Heme acquisition mechanisms of *Porphyromonas gingivalis* – strategies used in a polymicrobial community in a heme-limited host environment, *Mol Oral Microbiol* 32 (2017) 1–23.
- [41] K. Kuzelova, M. Mrhalova, Z. Hrkal, Kinetics of heme interaction with heme-binding proteins: the effect of heme aggregation state, *Biochim. Biophys. Acta* 1336 (1997) 497–501.
- [42] J.W. Smalley, J. Silver, P.J. Marsh, A.J. Birss, The periodontopathogen *Porphyromonas gingivalis* binds iron protoporphyrin IX in the mu-oxo dimeric form: an oxidative buffer and possible pathogenic mechanism, *Biochem. J.* 331 (Pt 3) (1998) 681–685.
- [43] P.S. Bhogal, N. Slakeski, E.C. Reynolds, A cell-associated protein complex of *Porphyromonas gingivalis* W50 composed of Arg- and Lys-specific cysteine proteinases and adhesins, *Microbiology* 143 (Pt 7) (1997) 2485–2495.

- [44] K. Nakayama, D.B. Ratnayake, T. Tsukuba, T. Kadokawa, K. Yamamoto, S. Fujimura, Haemoglobin receptor protein is intragenically encoded by the cysteine proteinase-encoding genes and the haemagglutinin-encoding gene of *Porphyromonas gingivalis*, *Mol. Microbiol.* 27 (1998) 51–61.
- [45] J. Potempa, A. Sroka, T. Imamura, J. Travis, Gingipains, the major cysteine proteinases and virulence factors of *Porphyromonas gingivalis*: structure, function and assembly of multidomain protein complexes, *Curr. Protein Pept. Sci.* 4 (2003) 397–407.
- [46] A.A. DeCarlo, M. Parameswaran, P.L. Yun, C. Collyer, N. Hunter, Porphyrin-mediated binding to hemoglobin by the HA2 domain of cysteine proteinases (gingipains) and hemagglutinins from the periodontal pathogen *Porphyromonas gingivalis*, *J. Bacteriol.* 181 (1999) 3784–3791.
- [47] J.W. Smalley, M.F. Thomas, A.J. Birss, R. Withnall, J. Silver, A combination of both arginine- and lysine-specific gingipain activity of *Porphyromonas gingivalis* is necessary for the generation of the micro-oxo bishaeam-containing pigment from haemoglobin, *Biochem. J.* 379 (2004) 833–840.
- [48] J.W. Smalley, A.J. Birss, B. Szmiigelski, J. Potempa, Sequential action of R- and K-specific gingipains of *Porphyromonas gingivalis* in the generation of the haem-containing pigment from oxyhaemoglobin, *Arch. Biochem. Biophys.* 465 (2007) 44–49.
- [49] M.S. Hargrove, D. Barrick, J.S. Olson, The association rate constant for heme binding to globin is independent of protein structure, *Biochemistry* 35 (1996) 11293–11299.
- [50] M.F. Perutz, Mechanisms regulating the reactions of human hemoglobin with oxygen and carbon monoxide, *Annu. Rev. Physiol.* 52 (1990) 1–25.
- [51] J.L. Gao, K.A. Nguyen, N. Hunter, Characterization of a hemophore-like protein from *Porphyromonas gingivalis*, *J. Biol. Chem.* 285 (2010) 40028–40038.
- [52] C.E. James, Y. Hasegawa, Y. Park, V. Yeung, G.D. Tribble, M. Kuboniwa, D. R. Demuth, R.J. Lamont, LuxS involvement in the regulation of genes coding for hemin and iron acquisition systems in *Porphyromonas gingivalis*, *Infect. Immun.* 74 (2006) 3834–3844.
- [53] S.A. Nicolaou, A.G. Fast, E. Nakamaru-Ogiso, E.T. Papoutsakis, Overexpression of *fetA* (*ybbL*) and *fetB* (*ybbM*), encoding an Iron exporter, enhances resistance to oxidative stress in *Escherichia coli*, *Appl. Environ. Microbiol.* 79 (2013) 7210–7219.
- [54] J. Wang, K. Pantopoulos, Regulation of cellular iron metabolism, *Biochem. J.* 434 (2011) 365–381.
- [55] P. Arosio, L. Elia, M. Poli, Ferritin, cellular iron storage and regulation, *IUBMB Life* 69 (2017) 414–422.
- [56] R. Spooner, O. Yilmaz, The role of reactive-oxygen-species in microbial persistence and inflammation, *Int. J. Mol. Sci.* 12 (2011) 334–352.
- [57] L.G. Henry, R.M. McKenzie, A. Robles, H.M. Fletcher, Oxidative stress resistance in *Porphyromonas gingivalis*, *Future Microbiol.* 7 (2012) 497–512.
- [58] S.G. Dashper, C.A. Butler, J.P. Lissel, R.A. Paolini, B. Hoffmann, P.D. Veith, N. M. O'Brien-Simpson, S.L. Snelgrove, J.T. Tsiros, E.C. Reynolds, A novel *Porphyromonas gingivalis* FeoB plays a role in manganese accumulation, *J. Biol. Chem.* 280 (2005) 28095–28102.
- [59] J. He, H. Miyazaki, C. Anaya, F. Yu, W.A. Yeudall, J.P. Lewis, Role of *Porphyromonas gingivalis* FeoB2 in metal uptake and oxidative stress protection, *Infect. Immun.* 74 (2006) 4214–4223.
- [60] M. Si, Y. Wang, B. Zhang, C. Zhao, Y. Kang, H. Bai, D. Wei, L. Zhu, L. Zhang, T. G. Dong, X. Shen, The type VI secretion system engages a redox-regulated dual-functional Heme transporter for zinc acquisition, *Cell Rep.* 20 (2017) 949–959.
- [61] P. Korbashi, J. Katzhendler, P. Saltman, M. Chevion, Zinc protects *Escherichia coli* against copper-mediated paraquat-induced damage, *J. Biol. Chem.* 264 (1989) 8479–8482.